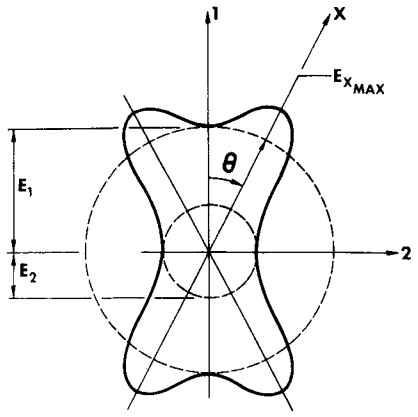

Fig. 2 Variation of Young's modulus, E_x, with rotation from principal material directions for an orthotropic material with high G_{12}.

$$\gamma_{xy}/2 = -(m_x/2E_1)\sigma_x - (m_x/2E_1)\sigma_y + (1/2G_{xy})\tau_{xy} \quad (7)$$

Also, Chu's Eq. (11) should read

$$\frac{d(E_1/E_x)}{d\theta} = -4(1-a-4b)\cos^3\theta\sin\theta - 2(4b-2a)\sin\theta\cos\theta = 0 \quad (8)$$

The foregoing results can be summarized by the observation that an orthotropic material can have an apparent Young's modulus in nonprincipal material directions that either exceeds or is less than the Young's moduli in both principal material directions. The graphical interpretation of Eqs. (4) and (5) with accompanying restrictions is shown in Fig. 1. The "intuitively predicted" variation of E_x with θ is given by the curve labeled

$$E_1/[2(1+\nu_{12})] \geqq G_{12} \geqq E_1/[2(E_1/E_2+\nu_{12})] \quad (9)$$

The visual impact of Fig. 1 is unavoidable; this graphical display is particularly effective in illustrating the three types of behavior ["high," "medium," and "low" G_{12} for Eqs. (4, 9, and 5), respectively].

Physically, the results mean that the shearing modulus of an orthotropic material has a strong influence on the character of the Young's moduli in nonprincipal material directions. If G_{12} is low as in woven materials, then E_x at say $\theta = 45°$ will be lower than E_2. For example, pull on an ordinary pillow case or bedsheet in the two orthogonal fiber directions and then at 45° to the fibers. In the latter case, E_x is sensibly much lower than either E_1 or E_2. A structurally more practical but less vivid example of a "low" G_{12} material is boron/epoxy with material properties.

$$E_1 = 30\times10^6 \text{ psi} \quad E_2 = 3\times10^6 \text{ psi} \quad G_{12} = 1\times10^6 \text{ psi}$$
$$\nu_{12} = 0.3$$

Obviously, Eq. (5) is satisfied, but the inequality is not strong so the minimum value of E_x is only slightly less than E_2. Examples of the intermediate behavior ("medium" G_{12}) characterized by Eq. (9) include glass/epoxy and high modulus graphite/epoxy although their shear moduli are nearly low enough to qualify them as "low" G_{12} materials. Apparently, Chu's extensionally orthotropic laminate has a "high" value of G_{12} such that Eq. (4) is satisfied although he did not give any material properties. Generally, "high" G_{12} materials will not occur naturally and will not likely occur with woven materials because the matrix material is usually quite flexible and hence has a low G itself. Thus, the composite has a low G_{12} since the matrix shear modulus is the dominant influence on the composite shear modulus. Apparently, one of the few practical ways of achieving "high" G_{12} materials is to increase G_{12} for a composite not by increasing G of the matrix material but by adding angle-ply layers to increase A_{66}, the laminate shearing stiffness. However, this possibility often involves more than just an orthotropic material; care must be taken to perform an adequate laminate analysis.

Note that orthotropic materials with either high or low G_{12} do not have their largest and smallest Young's moduli in orthogonal directions as do orthotropic materials with medium G_{12}. As an example, consider E_x for an orthotropic material with high G_{12} shown in Fig. 2 for a complete revolution in observation angle. There, the largest E_x values occur at roughly $\theta = \pm30°$ and $\theta = \pm150°$ with the smallest E_x values at $\theta = \pm90°$. Thus, not only are there nonorthogonal directions for maximum and minimum values, but the maximum occurs at *four* values of θ instead of only two as for materials with medium G_{12}. The significance of principal material axes is that they are axes of *material symmetry* but do not necessarily coincide with maximum or minimum values of the material properties.

Conclusions

Laminated composite materials must be completely specified as to stacking sequence, number and orientation of layers, and lamina material properties because of the complex nature of the laminate stiffness A_{ij}, B_{ij}, and D_{ij}. Care must be taken to use proper terminology resulting from a laminate analysis to avoid misleading nomenclature.

Orthotropic materials, at arbitrary observation angles, can have larger or smaller values of the Young's modulus E_x than E_1 or E_2, the Young's moduli in principal material directions. The values of E_x depend on the value of the shearing modulus in principal material coordinates, G_{12}. Practical examples of materials with low, medium, and high G_{12} are given.

References

[1] Chu, K. S., "Some Characteristics of Laminated Filamentary Composites," *AIAA Journal*, Vol. 9, No. 7, July 1971, pp. 1407–1408.

[2] Ashton, J. E., Halpin, J. C., and Petit, P. H., *Primer on Composite Materials: Analysis*, Technomic, Westport, Conn., 1969.

[3] Lovelace, A. M. and Tsai, S. W., "Composites Enter the Mainstream of Aerospace Vehicle Design," *Astronautics and Aeronautics*, Vol. 8, No. 7, July 1970, pp. 56–61.

Char Formation in Ablatives

R. P. RASTOGI* AND DESH DEEPAK†
Gorakhpur University, Gorakhpur (U.P.), India

CHARRING ablators have been employed as a heat shield during re-entry of space capsules[1] and for protection of rocket nozzles. Such ablators usually decompose to form porous carbon (char) and low molecular weight gases. Heat protection of the space vehicle is provided[2] by a) conductive heat transfer through the char and convective heat transfer through the entrapped volatile products, b) transpiration, c) endothermic chemical reaction of decomposition products, d) reradiation from the char front surface, and e) thickening of the boundary layer. In order to understand the nature of ablating boundary layer, detailed measurements under turbulent ablating conditions have been made recently[3] and the effect on surface heat transfer of gas phase chemical reactions involving ablation products have also been studied.[4] Many new types of ablating materials have been reported during recent years. However, it seems that the chemistry of char formation has not received the attention which it deserves. In this communication, we shall discuss the chemistry of char formation based on the nature of decomposition products and the bond energy considerations.

Received June 28, 1973. The authors are thankful to C.S.I.R. (India) for supporting the investigation.

Index categories: Material Ablation; Materials, Properties of; Spacecraft Temperature Control Systems.

* Professor of Chemistry. Associate Fellow AIAA.

† Research Fellow, Department of Chemistry.

Table 1 Data on typical ablatives

Polymer	Structure	% Composition				Char[5] yield, %
		C	O	N	H	
Conventional phenolic (phenol-formaldehyde)	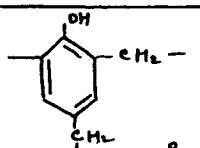	80.67	13.44	-	5.88	60.00
Polyimide	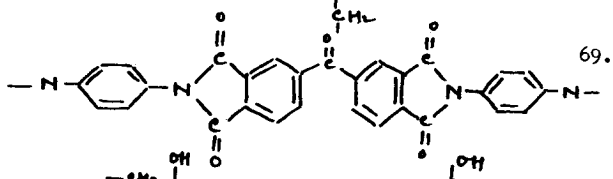	69.60	16.00	11.20	3.20	63.00
Napthalenediol phenol-formaldehyde	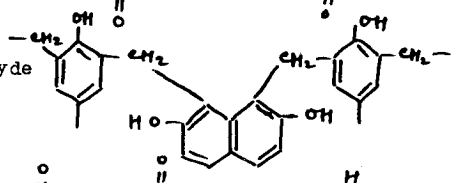	78.78	16.10	-	5.05	63.40
Polyamide-imide	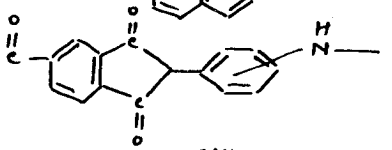	68.10	18.18	10.60	3.03	65.00
Biphenol-formaldehyde	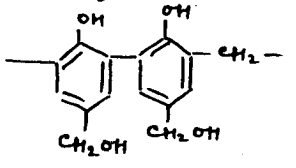	69.76	24.80	-	5.42	65.10
p-Phenylphenol phenol-formaldehyde	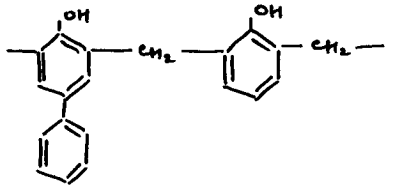	83.33	18.22	-	9.11	70.00
Polybenzimidazole	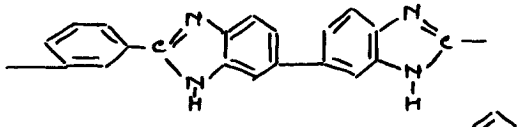	77.90	-	16.80	3.89	73.90
m-Polyphenylene (xylene glycol-cured)	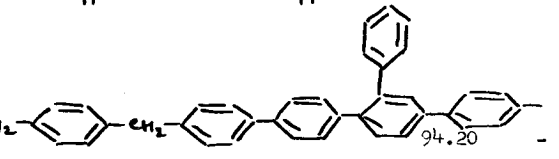	94.20	-	-	5.78	77.00

Char formation on heating polymers is simply the result of thermal degradation of polymers at high temperatures and specific environment. Initially, on pyrolysis, free radicals are formed. Further chain cleavage is propagated when a free radical abstracts a hydrogen atom and thus reaction starts. Chain termination occurs when two free radicals combine to form a neutral species. It has been suggested[1] for the formation of char that the rate of chain termination reaction should be greater than that for the chain cleavage reaction. Such a situation is favored by a cross-linked polymer. However, for getting a porous char, we need another polymer as companion for which the rate of chain cleavage reaction predominates so that large quantities of gaseous decomposition products are produced. For the former phenolic resins are to be preferred and for the latter nylon has been chosen so that nylon phenolics are more commonly used as ablatives.

We present below in Table 1 data on a few typical ablatives for discussion.

Bond energies of the bonds involved are given in Table 2.

Table 2 Bond energies[6] of a few typical bonds in k cal/mole at 25°C

Bond	Bond energy
C—N	72.8
C—C	82.6
C—O	85.5
N—H	93.4
C—H	98.7
O—H	110.6
C=C	145.8
C=N	147.0
C=O	179[a]
C≡C	199.6

[a] Ketone.

Conclusions

From Tables 1 and 2 it follows that a good ablative must satisfy the following requirements from chemical considerations: a) it should have a high carbon content, b) the percentage of oxygen should be lower in order to minimize the formation of CO or CO_2 and thus conserve carbon in the solid-state, c) since C=C and C≡C have higher bond energy, a larger percentage of these in the polymer chain would yield a good ablative, d) more of C—H bonds would be desirable since C—H bond is very weak and the rupture of the bond would yield hydrogen which has got a high specific heat, and e) the formation of low molecular weight gases on decomposition is desirable for getting larger concentration of pores per unit volume.

The aforementioned ideas, particularly c and e, are verified for the case of pyrolysis of phenolic resin. The composition of the gaseous products on pyrolysis at various temperatures has been reported by Rindal, Flood and Kendall[7] which confirms the belief that weaker bonds will break first on pyrolysis.

It should be noted that in the above analysis, the relative strength of the bonds has been assessed on the basis of given values of bond energy which refer to gaseous components of the reaction. In the present case, pyrolysis of solid into gaseous products is considered and hence the thermochemistry should involve heats of sublimation of certain species. It appears that the relative bond strengths would be unaffected even if this factor were taken into account and the postulated basis of the mechanism of pyrolysis remains intact.

References

[1] McAllister, L., Bolger, J., McGaffery, E., Roy, P., Ward, F., and Walker, A. C., Jr., "Ablative Materials for High-Temperature Thermal Protection of Space Vehicles," *Journal of Chemical Education*, Oct. 1971, p. 690.

[2] Gary, C. A., Pike, R. W., and Del Valle, E. G., "Modelling Reacting Gas Flow in the Char Layer of an Ablator," *AIAA Journal*, Vol. 9, No. 6, June 1971, pp. 1113–1119.

[3] Lipfert, E. and Genovese, J., "An Experimental Study of the Boundary Layers on Low-Temperature Subliming Ablators," *AIAA Journal*, Vol. 9, No. 7, July 1971, pp. 1330–1337.

[4] Mills, A. F., Gomez, A. V., and Strouhal, G., "Effect of Gas Phase Chemical Reactions On Heat Transfer to Charring Ablators," *Journal of Spacecraft and Rockets*, Vol. 8, No. 6, June 1971, pp. 618–625.

[5] Schmidt, D. L., "Ablative Polymers in Aerospace Technology," *Journal of Macromolecular Science—Chemistry*, Part A, Vol. 3, No. 3, May 1969, pp. 327–365.

[6] Roberts, J. D. and Caserio, M. C., *Modern Organic Chemistry*, W. A. Benjamin, Inc., New York, 1967, p. 65.

[7] Rindal, R. A., Flood, D. T., and Kendall, R. M., "Analytical and Experimental Study of Ablation Material for Rocket Engine Application," CR-54757, 1966, NASA.

Local Thermal Equilibrium in a Transient Arc

DAVID M. BENENSON* AND AUGUST A. CENKNER JR.†
State University of New York at Buffalo, Buffalo, N.Y.

EXPERIMENTS have been conducted upon a 1-cm-diam, 14-cm-length, coaxial cascade argon arc to obtain information on equilibrium during the dynamic response to an applied

Received July 25, 1973. This work was supported by National Science Foundation Grant GK-24292 and by U.S. Air Force Office of Scientific Research Grant 70-1928.

Index categories: Plasma Dynamics and MHD; Electric Power Generation Research.

* Professor, Faculty of Engineering and Applied Sciences. Associate Fellow AIAA.

† Research Assistant, Department of Engineering Science; presently with the Perkin-Elmer Corporation, Danbury, Conn.

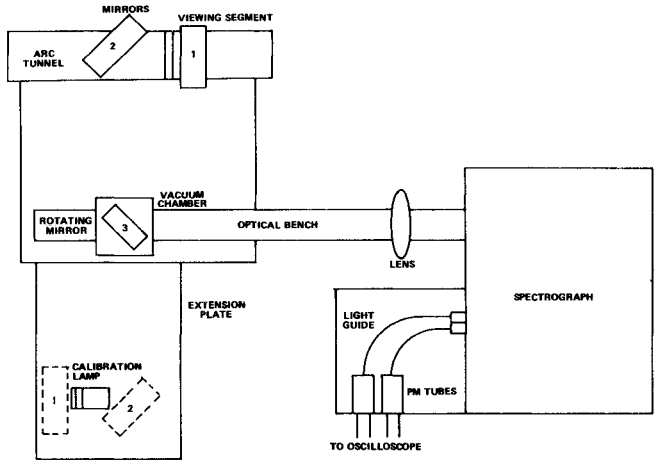

Fig. 1 Optical system.

(positive) voltage pulse. Tests were carried out at pressure levels of 510, 820, and 1120 torr. The arc was operated at initial steady-state currents of 195 amp, 180 amp, and 170 amp, at the respective pressures. The positive voltage pulse resulted in final steady-state current levels about 40 amp larger than initial values. Current rise times were about 400 μsec at all pressure levels; the applied voltage rise time was about 50 μsec. Argon mass flow rate was 0.1 g/s.

Arc radiation data were obtained through the use of an optical system (Fig. 1) containing a high-speed rotating mirror apparatus whose spatial positioning was synchronized with respect to the initiation of the voltage pulse. Data acquisition times were 5 μsec. The 4158.6 ArI line and the adjacent continuum radiation at 4143 Å were simultaneously monitored in the initial steady state and at 15, 30, 100, 200, and 1500 μsec following application

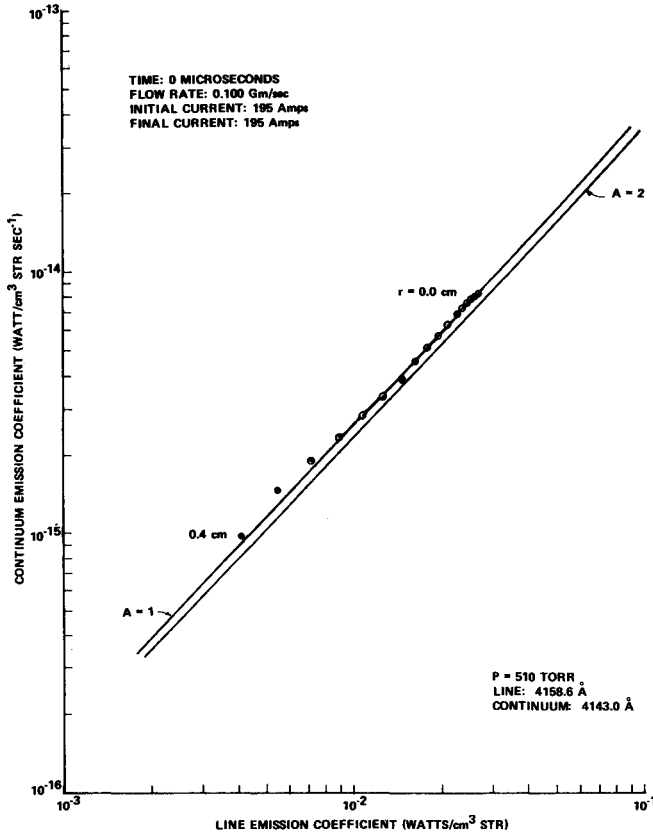

Fig. 2 Emission coefficients, initial steady state.